Numerical simulation of laser-generated Lamb wave by finite element method in thin transversely isotropic laminate composite

Jijun Wang (王纪俊)[1,2], Zhonghua Shen (沈中华)[1], Baiqiang Xu (许伯强)[2], Xiaowu Ni (倪晓武)[1], Jianfei Guan (关建飞)[1], and Jian Lu (陆 建)[1]

[1] *Department of Applied Physics, Nanjing University of Science and Technology, Nanjing 210094*
[2] *Faculty of Science, Jiangsu University, Zhenjiang 212013*

Laser ultrasound is a technique based on lasers to generate and detect ultrasound remotely. The thermal expansion arising from the optical absorption of a short laser pulse generates ultrasonic wave. By using finite element method, this study presents a source model for laser ultrasonic generation in thin transversely isotropic laminate composite in the thermoelastic regime. According to the thermoelastic theory, the transient temperature is equivalent to a body source to generate ultrasonic waves. The numerical results indicate that the symmetric and antisymmetric Lamb wave is excited in thin transversely isotropic laminate composite plate, the evolution of the dispersive waveform is a function of the source-receiver distance, the plate thickness, and the parameters of the fiber-reinforced composite. These results are very useful for evaluation materials parameters of the composite plate.

OCIS codes: 110.7170, 350.7420.

Fiber-reinforced composite materials have been utilized extensively in industrial applications, such as ship and aircraft engineering. However, the complex constitutive nature of composite materials leads to difficulties in the determination of their mechanical properties[1]. Due to its noncontact feature and the ability of broadband signal generation, laser ultrasound has demonstrated its great potential for nondestructive evaluation[2,3].

Laser-generated transient Lamb waves can be used to estimate the thickness and elastic constants. Dewhurst[3] initiated that this method extracts the thickness of thin metal sheet. Hutchins[4], Bobbin[5] and Deschamps[6] have used this technique to measure the thickness and elastic constants in thin materials. Scudder[7] studied Lamb waves in fiber-reinforced composite plates with laser-based generation and detection. Cheng and Berthelot[8] investigated the laser generation of Lamb waves in orthotropic plates. Spicer[9] presented a theoretical formulation for laser ultrasonic wave generation in an isotropic thin plate by using the numerical inversion of the Hankel–Laplace transform solution. Dubois[10] developed a model of the thermoelastic excitation of ultrasound in an orthotropic thick plate based on temporal Laplace and spatial two-dimensional Fourier transforms for materials having orthotropic symmetry. Cheng[8] proposed that the normal mode expansion method for modeling the thermoelastic generation process of elastic wave forms in anisotropic plate or orthotropic plate.

Due to the complexity of the generation of the thermoelastic waves, numerical methods will be much more suitable in dealing with such complicated processes, especially the process where the material parameters are temperature dependent. The finite element method (FEM) is versatile due to its flexibility in modeling complicated geometry and its capability in obtaining full field numerical solutions. In this article, the models for thermal conductive equation and thermo-elastic mechanism generation equation in fiber-reinforced composite plate, transversely isotropic, are built by using FEM. The transient temperature and temperature gradient field are calculated, and the laser-generated transient Lamb waves are obtained. The influence of the thickness of specimen on the transient Lamb waves is analyzed.

The physical problem which we wish to consider is the structural response of a thin fiber-reinforced composite plate illuminated by a laser line source in normal direction. The geometry of the problem is shown in Fig. 1.

The classical thermal conduction equation for finite elements with the heat capacity matrix $[C_T]$, the conductivity matrix $[K]$, the heat flux vector $\{p_1\}$ and the heat source vector $\{p_2\}$ can be expressed as

$$[K]\{T\} + [C_T]\left\{\dot{T}\right\} = \{p_1\} + \{p_2\}, \tag{1}$$

where $\{T\}$ is the temperature vector, and $\{\dot{T}\}$ is the temperature rise rate vector.

For wave propagation, ignoring damping, the governing finite element equation is

$$[M]\{\ddot{\mathbf{U}}\} + [K]\{\mathbf{U}\} = \{\mathrm{F}_{\mathrm{ext}}\}, \tag{2}$$

where $[M]$ is the mass matrix, $[K]$ is the stiffness matrix, $\{\mathbf{U}\}$ is the displacement vector, $\{\ddot{\mathbf{U}}\}$ is the acceleration vector and $\{\mathbf{F}_{\mathrm{ext}}\}$ is the external force vector. For thermoelasticity, the external force vector for an element is $\int_{V_e} [B]^T[C]\{\varepsilon_0\}\mathrm{d}V$, where $\{\varepsilon_0\}$ is the thermal strain vector, $[\mathrm{B}]^T$ is the transpose of the derivative of the shape functions and $[C]$ is the material matrix.

A fiber-reinforced composite thin plate can be assumed

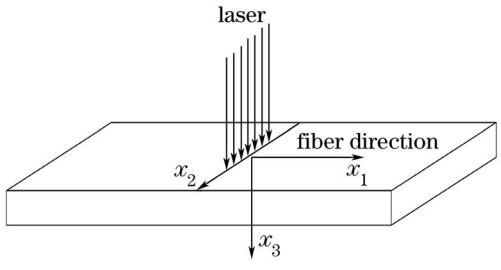

Fig. 1. Schematic diagram of laser irradiation.

as in transversely isotropic symmetry, and hence, the independent elastic constants are reduced from nine (orthotropic) to five. Let the x_1-axis be pointed along the fiber direction, then the x_2–x_3 plane is the isotropic plane (Fig. 1). The non-vanishing elastic constants are

$$[C_{ij}] = \begin{bmatrix} C_{11} & C_{12} & C_{12} & 0 & 0 & 0 \\ C_{12} & C_{22} & C_{23} & 0 & 0 & 0 \\ C_{12} & C_{23} & C_{22} & 0 & 0 & 0 \\ 0 & 0 & 0 & C_{44} & 0 & 0 \\ 0 & 0 & 0 & 0 & C_{55} & 0 \\ 0 & 0 & 0 & 0 & 0 & C_{55} \end{bmatrix}. \quad (3)$$

When the laser line direction is perpendicular to the fiber direction (shown in Fig. 1), plane Lamb waves are propagating in the x_1 direction with particle motion in the x_2-x_3 plane; whereas, when the laser line direction is parallel to the fiber direction, plane Lamb waves are propagating in the x_2 direction with particle motion in the x_1-x_3 plane. So a plane element model can be used to solve in these situations, shown in Fig. 2.

Based on the above-described models, the thermoelastically generated waves are calculated in a thin fiber-reinforced composite plate. The finite element mesh arrangement is shown in Fig. 2. The element length is 20 μm. The thickness of the fiber-reinforced composite plate is from 40 to 400 μm. The laser energy is 13.5 mJ and the pulse rise time t_0 and the radius of the pulsed laser spot on the sample surface are taken to be 10 ns and 300 μm, respectively. The properties of materials used in the calculation are listed in Table 1.

When the thin fiber-reinforced composite plate is illuminated by a laser line with the energy less than the melting threshold of the specimen, the energy of the laser pulse will be absorbed by the specimen, a transient temperature field and a transient temperature gradient field will be generated in the specimen[11], followed by the local thermal expansion. This thermal expansion induces ultrasonic waves in the thin plate.

Figure 3 shows the normal displacement waveforms of Lamb wave propagating parallel to the fiber direction, the source-receiver distance varies from 4 to 12 mm, and the plate thickness is 100 μm. The waveforms of Lamb wave propagating normal to the fiber direction are shown in Fig. 4. The results show that the lower frequency components of the a_0 and s_0 modes are dominant in such a thin plate. The symmetric mode (s_0 mode) arrives earlier than the antisymmetric mode (a_0 mode), while the amplitude of the symmetric mode is much smaller than that of the antisymmetric mode. The s_0 mode exhibits a non-dispersive spike, while the dispersive nature of the signal is very clear in the antisymmetric mode signals, i.e. higher frequency signal arrives earlier than lower frequency signal.

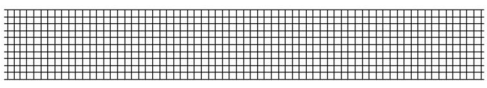

Fig. 2. Finite element meshes.

Table 1. Parameters Used in the Calculation

Thermal Conductive Coefficient K (W/(m · K))	1.6878	D_{11}(GPa)	50.34
Density ρ (kg/m^3)	1650	D_{22}(GPa)	18.22
Thermal Capacity C (J/(kg · K))	840	D_{12}(GPa)	2.45
Young's Modulus (Pa)	E_1=50.00 E_2=13.79	D_{23}(GPa)	8.94
Thermal Expansion Coefficient	α_{11}=0.31×10^{-5} α_{22}=0.10×10^{-6}	D_{55}(GPa)	4.54

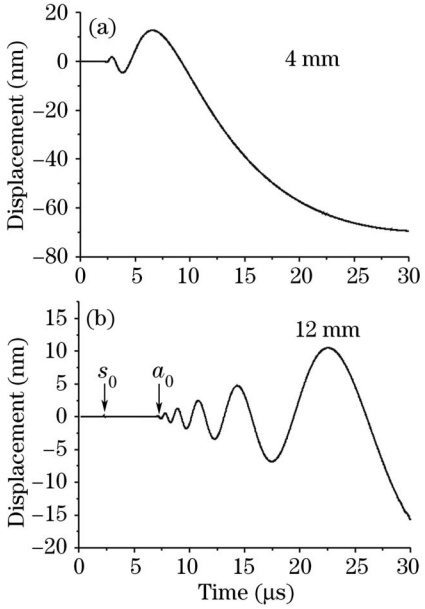

Fig. 3. The normal displacements at different source-receiver distances in the 100-μm-thick plate with propagating direction parallel to the fiber direction.

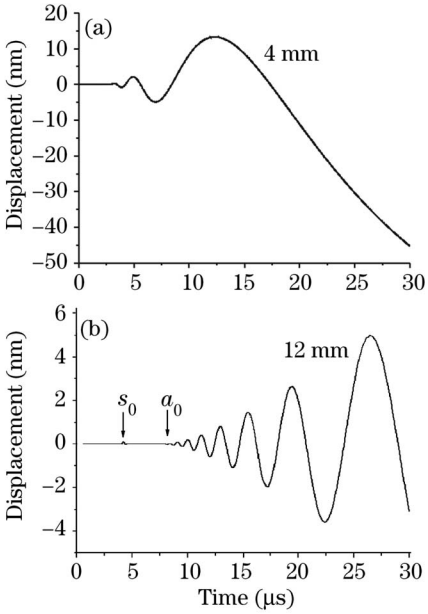

Fig. 4. The normal displacements at different source-receiver distances in the 100-μm-thick plate with propagating direction perpendicular to the fiber direction.

Comparing Fig. 3 and Fig. 4, one can find two distinct differences. The velocity of symmetric mode (s_0 mode) propagating parallel to the fiber direction is faster than the velocity propagating perpendicular to the fiber direction. The velocity of antisymmetric mode (a_0 mode) is similar. This is because the Young's modulus along the

fiber direction (E_1, shown in Fig. 1) is larger than E_2 (normal the fiber direction). Another difference is the dispersive nature. The waveforms propagating direction perpendicular to the fiber direction shows more clear dispersive characteristics of the Lamb wave signal and the frequencies are higher than the frequencies propagating direction parallel to the fiber direction. The numerical results indicate that the evolution of the dispersive waveforms is a function of the source-receiver distance. The evolution of the dispersive waveform in Fig. 3 and 4 is a function of the source-receiver distance.

The influence of the thickness of the fiber-reinforced composite plate on the normal displacement waveform of laser-generated Lamb wave has been calculated, as shown in Figs. 5 and 6. Figure 5 shows the normal displacement waveform of Lamb wave propagating parallel to the fiber direction, the plate thickness varies from 40 to 400 μm, and the source-receiver distance is 8 mm. The waveforms of Lamb wave propagating normal to the fiber direction

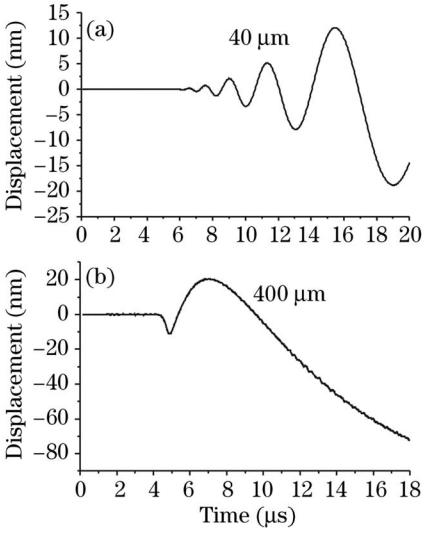

Fig. 5. The normal displacements in different thickness plate at source-receiver distance of 8 mm with propagating direction parallel to the fiber.

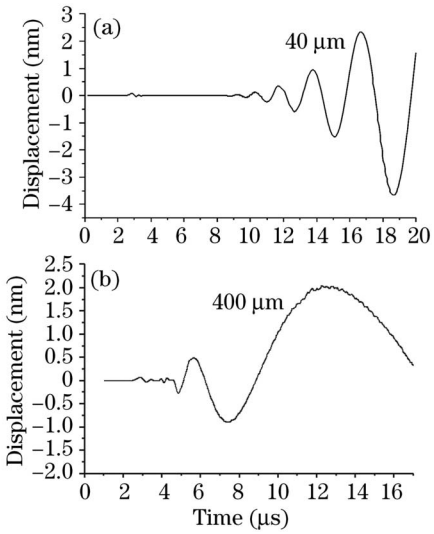

Fig. 6. The normal displacements in different thickness plate at source-receiver distance of 8 mm with propagating direction perpendicular to the fiber.

are shown in Fig. 6. The frequency of antisymmetric mode (a_0 mode) wave decreases and the waveform shows less dispersive characteristics of the Lamb wave signal with the thickness increases. This is because the phase velocity of the antisymmetric mode wave is relation to the product of frequency and thickness of the plate, so the frequency of antisymmetric mode (a_0 mode) wave decreases with the thickness increases.

In conclusion, the waveforms of the laser thermoelastically induced Lamb waves in thin fiber-reinforced composite plate are investigated by numerical simulation. The numerical results indicate that the evolution of the dispersive waveform is a function of the source-receiver distance and the plate thickness. The characteristics of Lamb waveforms, including velocity, amplitude and cutoff frequency, show anisotropic nature, also are functions of the parameters of the fiber-reinforced composite. The lower frequency components of the a_0 and s_0 modes are obtained. The velocity of Lamb wave (s_0 mode and a_0 mode) propagating parallel to the fiber direction is faster than the velocity propagating perpendicular to the fiber direction. The dispersive nature of Lamb waveform in two directions appears difference. These numerical results establish a quantitative relationship between the Lamb waveforms and the parameters of thin fiber-reinforced composite plate and laser input parameters, it is useful to laser-based technique for the non-destructive determination and evaluation of the thin fiber-reinforced composite plate.

This work was supported by the National Natural Science Foundation of China (No. 60208004), and partly supported by the Teaching and Research Award Program for Outstanding Young Professor in Higher Education Institute, MOE, P. R. China. X. Ni is the author to whom the correspondence should be addressed, his e-mail address is nxw@mail.njust.edu.cn.

References

1. R. M. Jones, *Mechanics of Composite Materials* (Scripta Book Company, Washington, 1975).
2. C. B. Scruby, R. J. Dewhurst, D. A. Hutchins, and S. B. Palmer, J. Appl. Phys. **51,** 6210 (1980).
3. R. J. Dewhurst, C. Edwards, A. D. W. Mckie. and S. B. Palmer, Appl. Phys. Lett. **51,** 1066 (1987).
4. D. A. Hutchins, K. Lundgren, and S. B. Palmer, J. Acoust. Soc. Am. **85,** 1441 (1989).
5. S. E. Bobbin, J. W. Wagner, and R. C. Cammarata, Ultrasonics **30,** 87 (1992).
6. M. Deschamps and O. Poncelet, J. Acoust. Soc. Am. **107,** 3120 (2000).
7. L. P. Scudder, D. A. Hutchins, and N. Guo, IEEE Trans. Ultrason. Ferroelectr. Freq. Control **43,** 870 (1996).
8. J. C. Cheng, S. Y. Zhang, and Y. H. Berthelot, *in Proceedings of 27th Annual Review of progress in Quantitative Nondestructive Evaluation* 1151 (2000).
9. J. B. Spicer, A. D. W. McKie, and J. W. Wagner, Appl. Phys. Lett. **57,** 1882 (1990).
10. M. Dubois, F. Enguehard, L. Bertrand, M. Choquet, and J. P. Monchalin, Appl. Phys. Lett. **64,** 554 (1994).
11. B. Q. Xu, Z. H. Shen, X. W. Ni, and J. Lu, J. Appl. Phys. **95,** 2116 (2004).